

# Knockdown of SASS6 reduces growth of MDA-MB-231 triple-negative breast cancer cells through arrest of the cell cycle at the G2/M phase

LILI DU<sup>1</sup>, JIEXIAN JING<sup>1</sup>, YAN WANG<sup>1</sup>, XIAOQIN XU<sup>1</sup>, TING SUN<sup>1</sup>, YANCHUN SHI<sup>1</sup>, WEIGANG WANG<sup>1</sup>, BAOGUO TIAN<sup>1</sup>, CUNZHI HAN<sup>1</sup>, XIANWEN ZHAO<sup>1</sup> and HUIBO CHANG<sup>2,3</sup>

<sup>1</sup>Department of Etiology, Shanxi Cancer Hospital, Taiyuan, Shanxi 030013; <sup>2</sup>Department of Biochemistry and Immunology; <sup>3</sup>Beijing Municipal Key Laboratory of Child Development and Nutriomics, Capital Institute of Pediatrics, Beijing 100020, P.R. China

Received February 20, 2020; Accepted March 18, 2021

DOI: 10.3892/or.2021.8052

**Abstract.** Spindle assembly abnormal protein 6 homolog (SASS6) is crucial for centriole duplication; however, the role of SASS6 in the proliferation of cancer cells remains unclear. In the present study, the expression and functional role of SASS6 in triple negative breast cancer (TNBC) was assessed. Immunohistochemical staining was performed using an anti-SASS6 antibody in TNBC and normal tissues. Lentivirus-mediated RNA interference was used to knock-down SASS6 in MDA-MB-231 TNBC cells. Cell viability was determined using an MTT assay, and cell cycle distribution and apoptosis were measured using flow cytometry. Additionally, PathScan intracellular signaling arrays were used to detect the presence of intracellular signaling molecules. The results revealed that SASS6 expression was increased in TNBC tissues compared with the control tissue. Moreover, SASS6 knock-down significantly suppressed the growth of MDA-MB-231 cells. MDA-MB-231 cell cycle progression was arrested at the G2/M phase and cyclin dependent kinase 1 (CDK1), cyclin B1 and PCNA expression in MDA-MB-231 cells was decreased following SASS6 knockdown. Furthermore, the phosphorylation of STAT3, BAD and rpS6 was reduced following SASS6 knockdown. A strong correlation between SASS6 and CDK1 expression was observed in TNBC tissues based on immunohistochemical staining analysis ( $R=0.989$ ;

$P<0.001$ ). In conclusion, the present study revealed the crucial role of SASS6 in promoting MDA-MB-231 cell growth, regulating cell cycle progression and its ability to downregulate the CDK1/cyclin B1 signaling pathway, thus highlighting the potential of SASS6 as a therapeutic target for treatment of TNBC, and merits further investigation in animal models or in preclinical and clinical studies.

## Introduction

Breast cancer is the most commonly diagnosed type of cancer in women worldwide. Triple negative breast cancer (TNBC) is defined as breast cancer lacking expression of specific hormone receptors, and is associated with a high degree of malignancy, a poor prognosis and drug resistance, and accounts for 15-20% of all breast cancer cases (1). Significant progress has been made in identifying oncogenes and tumor suppressor genes involved in the pathogenesis of breast cancer (2); however, the molecular mechanisms underlying this process remain poorly understood in TNBC. Therefore, novel and treatments are required to improve patient prognosis and survival.

Previous studies have revealed that centrosomes are associated with cancer development, as oncoproteins and tumor suppressor proteins are located in this organelle and drive aberrations in the centrosome (3-6). The centrosome is essential for cellular motility and intracellular transport, and centrosome defects can cause abnormal microtubule nucleation, formation of disorganized mitotic spindles, abnormal segregation of chromosomes and aneuploidy (7,8). Spindle assembly abnormal protein 6 homolog (SASS6) is an important centrosomal protein required for centrosome duplication (9). SASS6 serves an important role in the initiation of centriole formation and stabilization of centriole intermediates (10), and acts to ensure that each centriole seeds the formation of a single procentriole in each cell cycle. However, upregulated expression of SASS6 results in the seeding of more than one procentriole per centriole (11). It has recently been revealed that SASS6 expression is upregulated in several different types of cancer, often only modestly increased, including in invasive breast carcinomas, and SASS6 overexpression has been

*Correspondence to:* Professor Huibo Chang, Department of Biochemistry and Immunology, Capital Institute of Pediatrics, 2 Yabao Road, Beijing 100020, P.R. China  
E-mail: huibochang2012@163.com

Professor Jiexian Jing, Department of Etiology, Shanxi Cancer Hospital, 3 Zhigong New Road, Taiyuan, Shanxi 030013, P.R. China  
E-mail: 2912972872@qq.com

**Key words:** spindle assembly abnormal protein 6 homolog, knockdown, triple-negative breast cancer, G2/M phase arrest, cyclin dependent kinase 1, cyclin B1

revealed to cause excess foci-bearing centriolar markers in colorectal cancer (12). However, it is unclear whether SASS6 serves a role in TNBC.

To explore the role of SASS6 in human TNBC, expression analysis of SASS6 in TNBC tissues was performed by immunohistochemical staining, and then proliferation of human TNBC cells after SASS6 knocked out was analyzed by MTT method. The cell cycle distribution and apoptosis were detected by flow cytometry. Furthermore, the possible underlying mechanisms were assessed using PathScan intracellular signaling arrays and western blotting.

## Materials and methods

**Cell culture.** Human breast cancer cell lines MDA-MB-231, MDA-MB-468 and HCC-1937 cells (The Cell Bank of Type Culture Collection of the Chinese Academy of Sciences) were maintained in RPMI-1640 or DMEM (Gibco; Thermo Fisher Scientific, Inc.), supplemented with 10% (v/v) FBS, L-glutamine, a 2-fold vitamin solution (Gibco; Thermo Fisher Scientific, Inc.), 100 U/ml penicillin and 0.1 mg/ml streptomycin (Sangon Biotech, Co., Ltd.). Primary normal breast epithelial cells (PNBEC) were isolated from the unaffected contralateral breast of patients undergoing surgical procedures as previously described (13) and were cultured in DMEM/F12 supplemented with 5% FBS with antibiotics. All cells were maintained with 5% CO<sub>2</sub> at 37°C in a humidified incubator.

**Reverse transcription-quantitative (RT-q) PCR.** Total RNA was extracted from cells using TRIzol® (Invitrogen; Thermo Fisher Scientific, Inc.) according to the manufacturer's protocol. RNA was reverse-transcribed to cDNA by GoScript™ Reverse Transcription System (Promega Corporation) according to the manufacturer's procedure. Quantitative real-time PCR was performed on a Roche LightCycler 480 II Real-Time PCR platform using SYBRGreen MasterMix Kit (Takara Biotechnology Co., Ltd.) according to the manufacturer's instructions. The sequences of the primers used for amplification were: SASS6 forward, 5'-GCGGCTAATAAGAC TTAACCGA-3' and reverse, 5'-CTTCTTGCTTAGTCC GCTGTAG-3'; and GAPDH forward, 5'-TGACTTCAACAG CGACACCCA-3' and reverse, 5'-CACCTGTGTGCTGTA GCCAAA-3'. The thermocycling conditions for qPCR were: Denaturation at 95°C for 15 sec; followed by 45 cycles at 95°C for 5 sec and 60°C for 30 sec. All samples were assessed in triplicate. The 2<sup>-ΔΔC<sub>q</sub></sup> method (14) was used to calculate the relative expression of the gene of interest.

**Tissue samples and immunohistochemical staining.** TNBC tissue (n=18) and the matching normal breast tissue (n=18) were obtained as 4-μm paraffin-embedded tissue block slides from female patients diagnosed with TNBC who underwent surgery at Shanxi Cancer Hospital (Shanxi, China) between October 2003 and August 2007 (age range, 38-57 years). The use of tissues from patients was retrospective in the present study. TNBC patients did not receive any chemotherapy or endocrine therapy prior to tumour removal. Ethics approval was obtained from the Ethics Committee of Shanxi Cancer Hospital and written informed consent was obtained from each patient prior to sample collection. The slides were

deparaffinized, dehydrated, immersed in Tris-EDTA buffer (pH 9.0) and incubated at 4°C overnight with anti-SASS6 (dilution 1:400; cat. no. 21377-1-AP; ProteinTech Group, Inc.), and anti-cyclin dependent kinase 1 (CDK1) (dilution 1:400; cat. no. 19532-1-AP; ProteinTech Group, Inc.) separately, and subsequently incubated for 15 min at 37°C with a poly-horse-radish peroxidase anti-rabbit antibody (dilution 1:500; cat. no. SA00004-2; ProteinTech Group, Inc.). After visualization of the reaction using DAB as a chromogen (Shanghai Gene Technology Co., Ltd.), the slides were counterstained with hematoxylin for 30 sec at room temperature and mounted using glycerin gel. The expression of SASS6 and CDK1 in tissues was observed using a light microscope (magnification, x40; B41; Olympus Corporation). The results were evaluated and scored by two blinded pathologists. Expression in tissues was stratified as follows: <10%, -; 10-30%, +; 31-80%, ++; and >80%, +++.

**Recombinant lentiviral vector production and infection.** The complementary DNA sequence (5'-TGGCACTTTAGGAGC ATTA-3') of SASS6 and the control short hairpin (sh)RNA (shCtrl) sequence (5'-TTCTCCGAACGTGTCACGT-3') were designed and inserted into a pGCSIL-GFP lentiviral vector (Shanghai GeneChem Co., Ltd.), and the 3rd recombinant lentivirus was generated. To generate the 3rd recombinant lentivirus, the reconstructed SASS6 silencing plasmid/control plasmid (20 μg) and packaging vector (15 μg) and envelope vector (10 μg) were co-transfected into 293T cells (The Cell Bank of Type Culture Collection of the Chinese Academy of Sciences) using Lipofectamine 2000 according to the manufacturer's procedure. Approximately 72 h after transfection, recombinant lentivirus was harvested and purified by ultracentrifugation. Then, cells were cultured in 6-well plates for lentivirus infection, and the shSASS6-lentivirus or negative control lentivirus, was added at multiplicity of infection (MOI) of 10 for 4 h. Cells were observed under a fluorescence microscope (MicroPublisher 1X71; Olympus Corporation) after 72 h of infection, and cells were harvested after 120 h of infection to determine knockdown efficiency using western blotting and RT-qPCR.

**Western blotting.** The cultured cells were lysed in a buffer (100 mM Tris-HCl, pH 6.8, 2% mercaptoethanol, 4% SDS, 20% glycerin) containing 1 mM protein inhibitor, 1 mM phenylmethylsulfonyl fluoride and complete protease inhibitors cocktail (MedChemExpress) for 10-15 min on ice. The lysates were centrifuged at 12,000 x g at 4°C for 15 min and the supernatants were collected. The protein content was measured by bicinchoninic acid (BCA) method. Aliquots (20 μg total protein/lane for each sample) were loaded on a 12.5% SDS-gel, resolved using SDS-PAGE and transferred to PVDF membranes. After blocking the membranes with 5% non-fat milk for 1 h at room temperature, they were incubated with anti-GAPDH (cat. no. sc-32233; Santa Cruz Biotechnology, Technology, Inc.), anti-SASS6 and anti-CDK1 (cat. nos. 21377-1-AP and 19532-1-AP; ProteinTech, Group, Inc.), anti-S6 ribosomal protein (rpS6) and anti-BAD (product codes ab225676 and ab32445; Abcam, Inc.), anti-PCNA (product no. 2586), anti-STAT3 (product no. 9139), phosphorylated (p)-STAT3 (Thr705) (product no. 9145), p-BAD (Ser116)

(product no. 5284) and p-rpS6 (Ser235/236) (product no. 4858; all from Cell Signaling Technology, Inc.) at 4°C overnight followed by incubation with goat anti-rabbit/mouse IgG HRP-linked antibodies (cat. nos. 7074 and 7076; Cell Signaling Technology, Inc.) for 1 h at room temperature. The antibodies were used in the following dilutions: Anti-SASS6, anti-CDK1, anti-rpS6, anti-BAD, anti-p-BAD, anti-p-STAT3, anti-STAT3 (all 1:1,000); anti-PCNA, anti-GAPDH, anti-p-rpS6 (all 1:2,000). Anti-GAPDH protein was used as an internal control. The signals were visualized using enhanced chemiluminescence reagent (Beijing BioChange Co., Ltd.). The protein expression level was analyzed by ImageJ software 1.8.0 (National Institutes of Health).

**Cell growth assay.** Cells in the logarithmic phase of growth infected with either the shCtrl lentivirus or shSASS6 lentivirus were plated in 96-well plates (2,000 cells/well). The cells were maintained in RPMI-1640 medium supplemented with 10% FBS for 5 days. The number of cells were counted using Celigo® Image Cytometer (Nexcelom Bioscience LLC). In each well, ≥800 cells were counted, and the cell growth assay was performed in triplicate.

**MTT assay.** Cell proliferation was assessed using an MTT assay according to the manufacturer's protocol. Briefly, the MDA-MB-231 cells at a density of  $3 \times 10^3$  cells/well were seeded in 96-well plates and incubated at 37°C overnight. Then the cells were infected with shSASS6 lentivirus or shCtrl lentivirus. Cell proliferation was measured every 24 h using 0.5 mg/ml MTT solution at 37°C for 4 h. Subsequently, 100  $\mu$ l of dimethyl sulfoxide (Sigma-Aldrich; Merck KGaA) was added to each well after discarding the supernatants. The plates were read at 490 nm using an ELISA reader (Tecan Infinite; Tecan Group, Ltd.). Each experiment was performed in triplicate.

**Cell cycle distribution analysis.** Flow cytometry following propidium iodide staining was used to analyze cell cycle distribution. After 4 days of lentiviral infection, MDA-MB-231 cells were plated in 60-mm dishes ( $2 \times 10^5$  cells/well). The cells were collected and fixed in 70% ice-cold ethanol for 12 h at 4°C. Subsequently, cells were stained with 0.05 mg/ml propidium iodide containing 100 U/ml RNase A (Fermentas; Thermo Fisher Scientific, Inc.) in the dark at room temperature for 30 min. DNA content of samples was measured on a FACSAria flow cytometer (BD Biosciences). The data were analyzed by FlowJo 7.6.3 software (FlowJo LLC).

**Intracellular signaling array.** To investigate the intracellular signaling pathways following SASS6 knockdown, a PathScan intracellular signal array (product no. 7323; Cell Signaling Technology, Inc.) was used to detect the expression of intracellular signaling proteins according to the manufacturer's protocol.

**Caspase activity assay.** A caspase assay system (Promega Corporation) was used to detect Caspase3/7 activity. Cells were maintained at 37°C in a humidified incubator with 5% CO<sub>2</sub> in 96-well plates and then the activities of Caspase-3/7 were measured according to the manufacturer's protocol. The

Table I. Immunohistochemical staining of SASS6 expression in TNBC and paired normal tissues.

Tissue	No. of specimens	Positive level			P-value <sup>a</sup>
		+	++	+++	
TNBC	18	1	2	15	<0.001
Normal	18	8	8	2	

<sup>a</sup>Fisher's exact test. SASS6, spindle assembly abnormal protein 6 homolog; TNBC, triple negative breast cancer.

reaction products were detected using an M2009PR microplate reader (Tecan infinite; Tecan Group, Ltd.) for the measurement of luminescence. Experiments were performed at least three times in duplicate.

**Apoptosis analysis.** An FITC Annexin V Apoptosis Detection kit I (BD Biosciences) was used to measure the proportion of viable cells according to the manufacturer's protocol and analyzed using a FACScan flow cytometer. After 4 days of lentiviral infection, MDA-MB-231 cells ( $5 \times 10^5$  cells/sample) were harvested, washed using cold PBS, resuspended in Annexin V-binding buffer and stained using propidium iodide and FITC Annexin V in the dark at room temperature for 15 min. After incubating, all the samples were analyzed by FACScan flow cytometry (Beckton Dickinson; BD Biosciences).

**Statistical analysis.** Fisher's exact test was used compare differences in SASS6 expression between cancer tissues and paired paracarcinoma tissues. The SASS6 mRNA expression was analyzed with ANOVA followed by Dunnett's post hoc test. The statistical significance between two groups (shCtrl vs. shSASS6) was determined using a Student's t-test for raw data. Data are presented as the mean  $\pm$  standard deviation. Spearman's rank correlation coefficient analysis was used to analyze the correlation between SASS6 and CDK1 expression.  $P < 0.05$  was considered to indicate a statistically significant difference.

## Results

**SASS6 expression in TNBC tissues.** It has previously been reported that SASS6 mRNA expression levels are upregulated in invasive breast carcinoma compared with normal tissues based on data obtained from The Cancer Genome Atlas (10). To analyze the status of SASS6 expression in TNBC tissues, the expression levels of SASS6 in clinical TNBC tissues and paired normal tissues were determined using immunohistochemical staining. SASS6 expression levels in TNBC tissues were significantly higher compared with the normal tissues (Table I,  $P < 0.001$ ; Fig. 1B). Representative images of SASS6 staining are presented in Fig. 1A.

**Lentivirus-mediated knockdown of SASS6 in MDA-MB-231 TNBC cells.** To compare the expression levels of SASS6 in different TNBC cell lines, the levels of SASS6 mRNA were

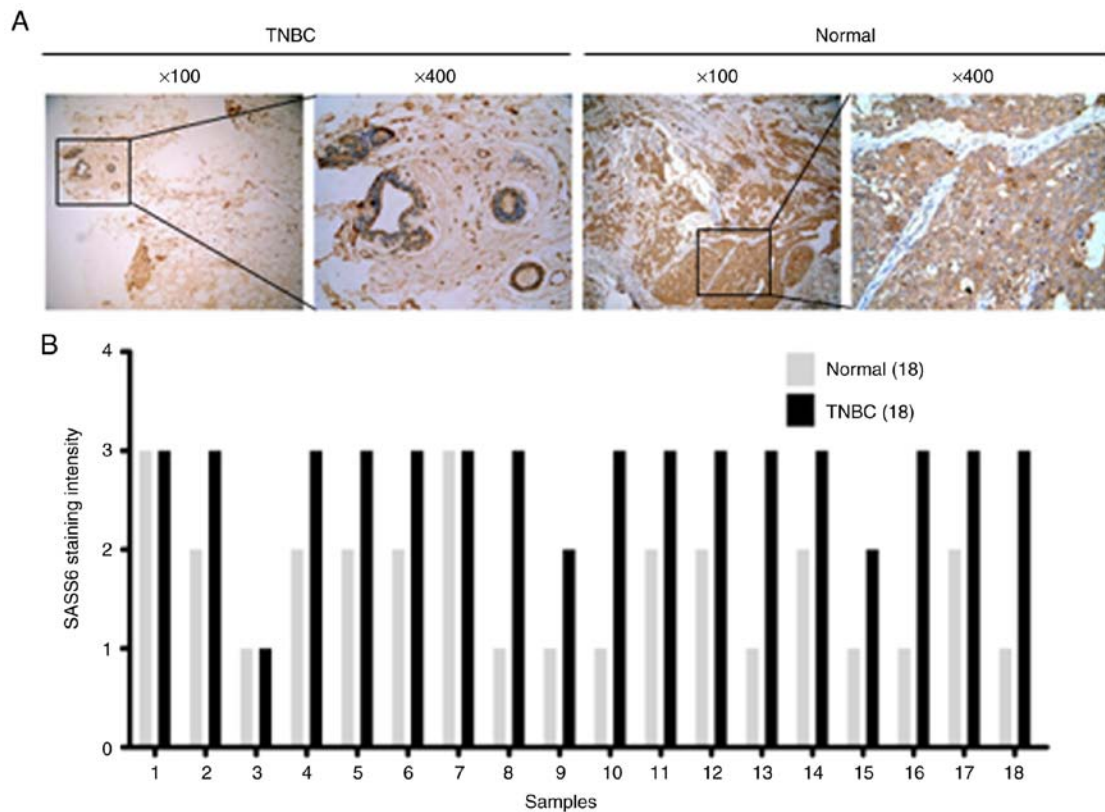


Figure 1. SASS6 expression levels in TNBC tissues. (A) Representative immunohistochemical images are presented of SASS6 expression in TNBC and paired normal breast tissues. (B) SASS6 expression was upregulated in TNBC tissues. TNBC, triple negative breast cancer; SASS6, spindle assembly abnormal protein 6 homolog.

detected in three TNBC cell lines. The results revealed that SASS6 mRNA expression was significantly increased in MDA-MB-231 and MDA-MB-468 cells compared with the PNBEC at the mRNA level ( $P < 0.01$ ; Fig. 2A). The MDA-MB-231 cells expressed higher levels of SASS6 expression compared with the HCC-1937 and MDA-MB-468 cells (Fig. 2A), and were thus used for the knockdown experiments, to explore the functional significance of SASS6. Lentiviral vectors are an efficient gene delivery method due to their unique ability to deliver target molecules into host cell DNA and replicate in non-dividing cells (15). Therefore, a control (shCtrl) and shSASS6 lentiviral vector was constructed. SASS6 knockdown was confirmed using RT-qPCR and western blotting in MDA-MB-231 cells. As revealed in Fig. 2B and C, SASS6 mRNA and protein expression levels were significantly reduced following transfection with SASS6-specific shRNA in MDA-MB-231 cells.

*SASS6 knockdown reduces the proliferation of breast cancer cells.* To observe the effect of SASS6 on cell growth, MDA-MB-231 cells infected with shSASS6 or shCtrl lentivirus were seeded into 96-well plates and subjected to 5 days of Celigo or MTT analysis. As shown in Fig. 2E, the knockdown of SASS6 significantly inhibited the growth of MDA-MB-231 cells. The MTT assay on MDA-MB-231 cells further revealed that during the 5 days, the control-transfected cells grew notably faster than the shSASS6-transfected cells (Fig. 2E). These data revealed that SASS6 knockdown potently suppressed cell proliferation of breast cancer cells.

*SASS6 knockdown arrests cell cycle progression of MDA-MB-231 cells at the G2/M phase and downregulates the expression of cell cycle-related proteins.* To study the mechanism by which SASS6 knockdown reduced growth, cell cycle distribution of MDA-MB-231 cells was detected using a flow cytometer. As revealed in Fig. 3A and B, the proportion of cells in the G0/G1 phase of the shSASS6-treated cells was lower than the shCtrl-treated cells ( $P < 0.01$ ), whereas the proportion of cells in the G2/M phase was increased ( $P < 0.01$ ). The percentage of cells in the G2/M phase was increased from  $11.34 \pm 2.19\%$  in the shCtrl-treated cells to  $43.19 \pm 3.28\%$  in the shSASS6-treated cells, indicating an arrest of cell cycle progression at the G2/M phase (Fig. 3A and B). These data indicated that cell cycle arrest served an important role in growth inhibition of breast cancer cells, and highlighted the involvement of SASS6 in this process.

In order to further determine the potential mechanism of G2/M-phase arrest, western blot analysis was used to detect the changes in the expression of cell cycle regulators in MDA-MB-231 cells following SASS6 knockdown. As revealed in Fig. 3C, in the shSASS6 treatment group, the expression levels of CDK1 and cyclin B1, which are associated with the G2-M transition were reduced, and PCNA expression was also reduced.

*CDK1 is overexpressed in TNBC tissues and is positively correlated with SASS6 expression.* The expression of CDK1, a potential downstream signaling molecule of SASS6 was investigated, and the relationship between CDK1 and SASS6 was determined. CDK1 expression levels in TNBC tissues

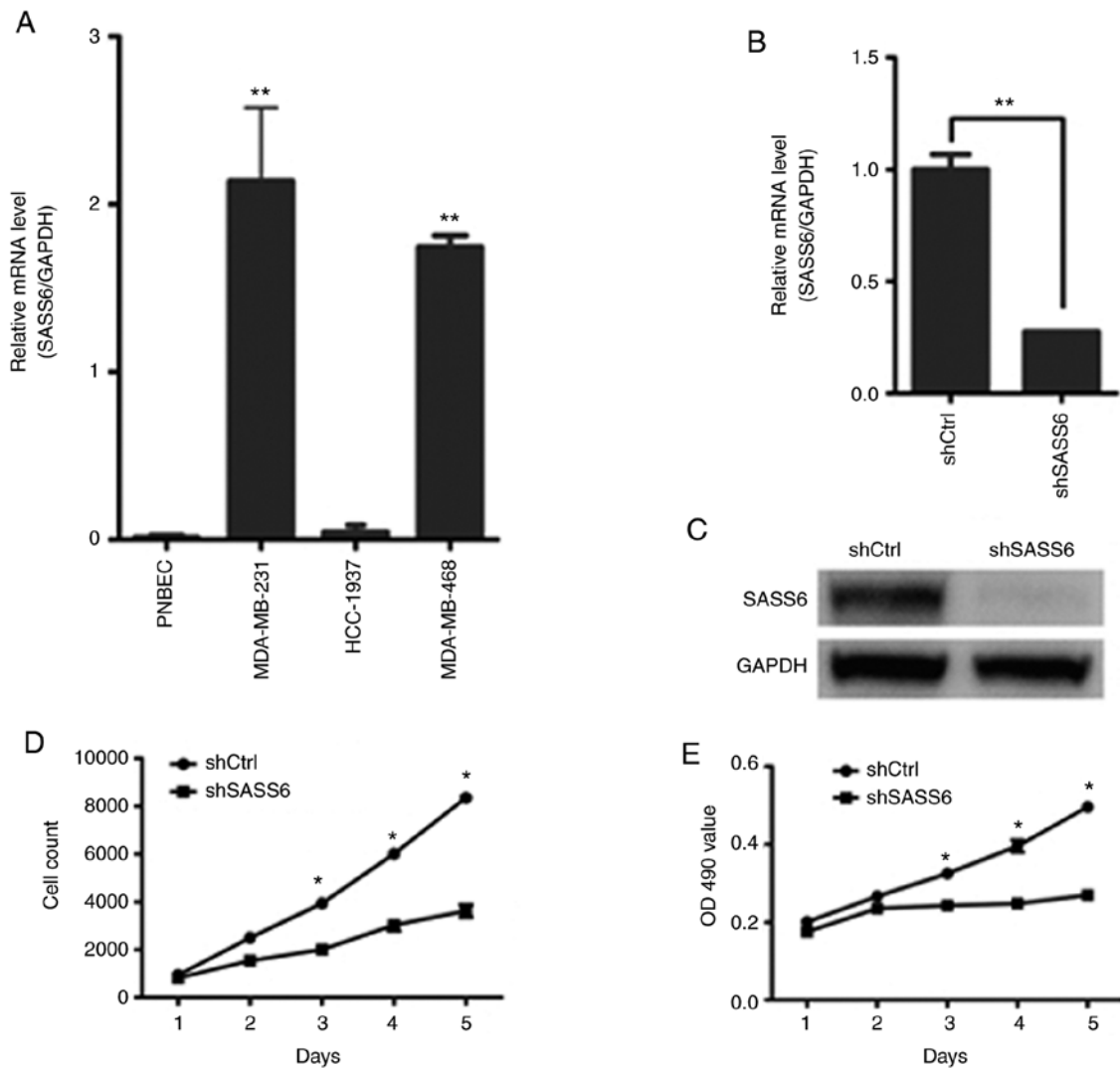


Figure 2. Effects of SASS6 knockdown on MDA-MB-231 cells. (A) mRNA expression levels of SASS6 were detected in the triple negative breast cancer cell lines and PNBEC. GAPDH expression was used as the internal control. \*\* $P < 0.01$  vs. PNBEC normal cells. (B) mRNA and (C) protein expression levels of SASS6 following transfection with shCtrl or shSASS6 5 days after infection. \*\* $P < 0.01$  vs. shCtrl. (D) Number of MDA-MB-231 cells were notably reduced following SASS6 knockdown. (E) MTT assays indicated that SASS6 knockdown significantly suppressed MDA-MB-231 cell viability.  $n=3$ . \* $P < 0.05$  vs. shCtrl. SASS6, spindle assembly abnormal protein 6 homolog; PNBEC, primary normal breast epithelial cells; sh, short hairpin; Ctrl, control.

Table II. Immunohistochemical staining of CDK1 expression in TNBC and paired normal tissues.

Tissue	No. of specimens	Positive level				P-value <sup>a</sup>
		+/-	+	++	+++	
TNBC	18	0	1	2	15	0.002
Normal	18	2	4	8	2	

<sup>a</sup>Fisher's exact test. CDK1, cyclin dependent kinase 1; TNBC, triple negative breast cancer.

were significantly higher compared with the normal tissues (Table II,  $P=0.002$ ; Fig. 4B). Representative images of SASS6 staining are presented in Fig. 4A. In addition, as revealed in Table III, SASS6 expression was positively correlated with CDK1 expression ( $R=0.989$ ;  $P<0.001$ ), suggesting a strong correlation between SASS6 and CDK1 expression in TNBC,

providing evidence at an *in vivo* level that SASS6 may regulate cell cycle progression in TNBC.

**Effects of SASS6 knockdown on STAT3, BAD and rpS6 protein phosphorylation.** To further elucidate the molecular mechanism by which SASS6 reduced breast cancer cell



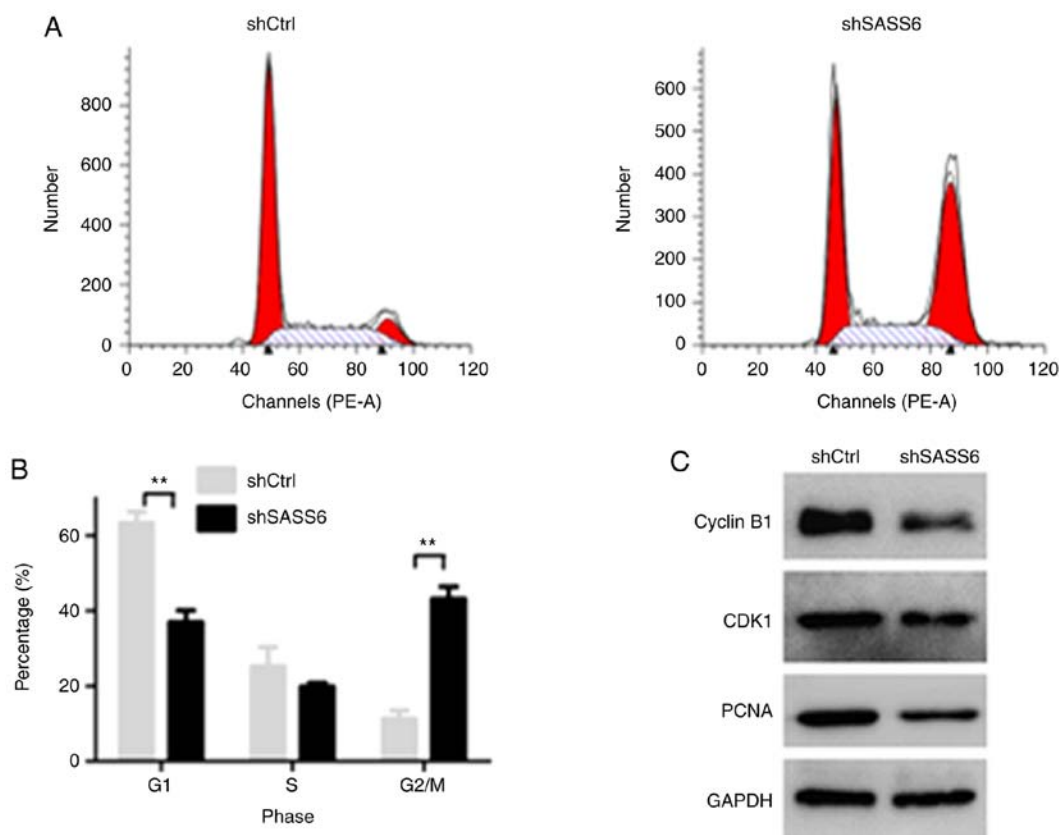


Figure 3. Effects of SASS6 knockdown on cell cycle progression of MDA-MB-231 cells. (A) Representative images of cell cycle distribution were acquired using flow cytometry. (B) Proportion of cells in the G0/G1, S and G2/M phases in cells infected with shCtrl or shSASS6 were analyzed. Data are presented as the mean  $\pm$  standard deviation of three independent experiments performed in triplicate. \*\* $P < 0.01$ . (C) Differences in protein expression levels of cyclin B1, CDK1 and PCNA between shSASS6 and shCtrl groups were determined using western blotting. SASS6, spindle assembly abnormal protein 6 homolog; CDK1, cyclin dependent kinase 1; PCNA, proliferating cell nuclear antigen; sh, short hairpin; Ctrl, control.

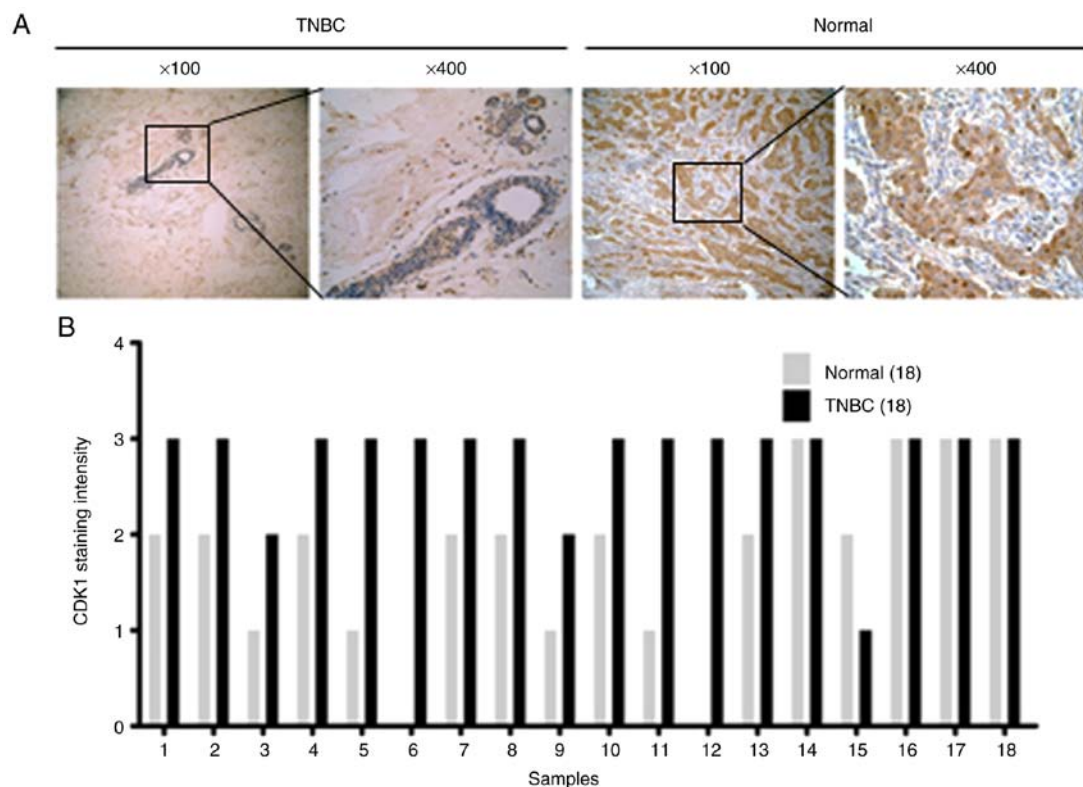


Figure 4. CDK1 expression levels in TNBC tissues. (A) Representative immunohistochemical images of CDK1 expression in TNBC and paired normal breast tissues. (B) CDK1 expression was upregulated in TNBC tissue. TNBC, triple negative breast cancer; CDK1, cyclin dependent kinase 1.

Table III. SASS6 expression is positively correlated with CDK1 expression in TNBC tissues (n=18).

Expression of CDK1	Expression of SASS6			R	P-value
	+	++	+++		
+	0	1	0	0.989	<0.001
++	1	1	0		
+++	0	0	15		

SASS6, spindle assembly abnormal protein 6 homolog; CDK1, cyclin dependent kinase 1; TNBC, triple negative breast cancer; R, r value of Spearman's correlation.

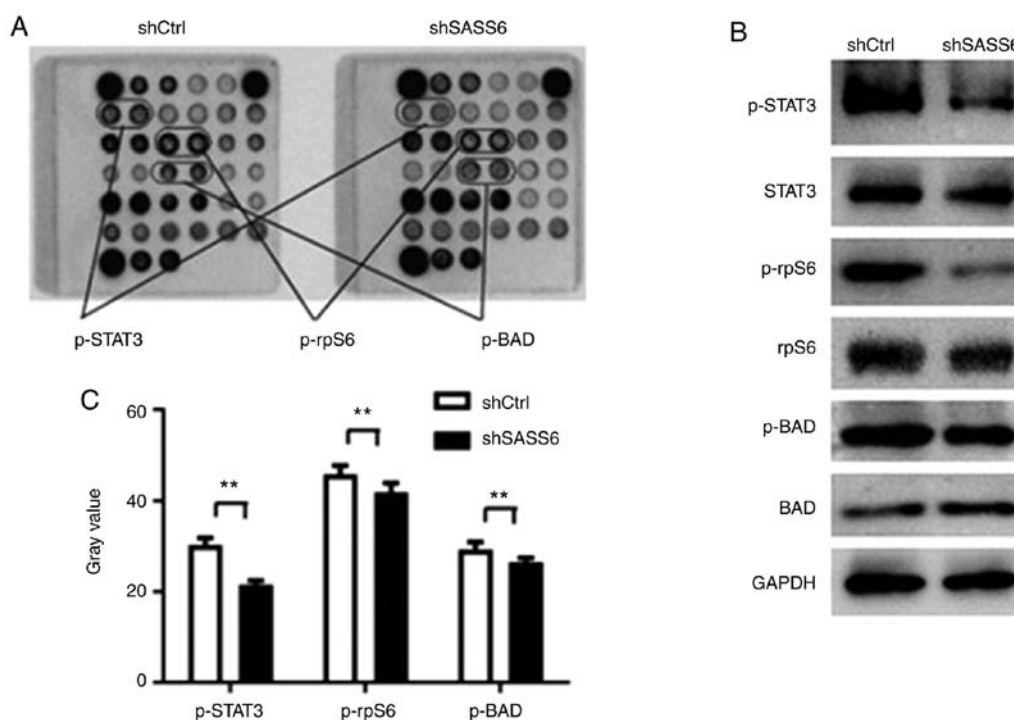


Figure 5. Effects of shSASS6 on the expression of multiple signaling molecules in MDA-MB-231 cells. (A) Representative images of intracellular signaling arrays are presented for shCtrl- and shSASS6-treated cells. (B) Quantitative analysis in the arrays revealed that the p-STAT3, p-rpS6 and p-BAD expression levels were decreased following SASS6 knockdown. n=3. \*\*P<0.01. (C) Western blot analysis of p-STAT3, STAT3, p-rpS6, rpS6, p-BAD and BAD expression in MDA-MB-231 cells transfected with shCtrl and shSASS6. SASS6, spindle assembly abnormal protein 6 homolog; sh, short hairpin; Ctrl, control; p-, phosphorylated; rpS6, S6 ribosomal protein.

growth, intracellular signaling arrays were used to analyze changes in the levels of signaling molecules in MDA-MB-231 cells following SASS6 knockdown. As revealed in Fig. 5A and B, the phosphorylation of STAT3 (Thr705), BAD (Ser116) and rpS6 (Ser235/236), was downregulated in shSASS6-treated cells (P<0.01). Subsequently p-STAT3 (Thr705), STAT3, p-rpS6, rpS6, p-BAD and BAD protein expression levels were determined using western blotting (Fig. 5C). The results revealed that SASS6 knockdown reduced the phosphorylation of STAT3, BAD and rpS6. These results supported the hypothesis that SASS6 serves a crucial role in TNBC cell growth by blocking the activation of STAT3 and rpS6 protein.

*Knockdown of SASS6 induces apoptosis of MDA-MB-231 cells.* BAD, a proapoptotic Bcl-2 family member, serves

an important role in apoptosis (16). Knockdown of SASS6 inhibited the phosphorylation of BAD, therefore, whether SASS6 affected apoptosis was next determined. Caspase3/7 analysis was performed following knockdown of SASS6 in MDA-MB-231 cells to determine this. The results revealed that the Caspase3/7 activity in MDA-MB-231 cells infected with shSASS6 lentivirus was significantly higher compared with the control group (P<0.01; Fig. 6A).

Knockdown of SASS6-induced apoptosis was further confirmed by staining cells with Annexin-V and propidium iodide. Consistent with the Caspase3/7 analysis, the results revealed that shSASS6-treated cells exhibited a significantly increased proportion of cells in early (lower right) and late (upper right) apoptosis (P<0.01; Fig. 6B and C). These results indicated that knockdown of SASS6 induced apoptosis in MDA-MB-231 cells.

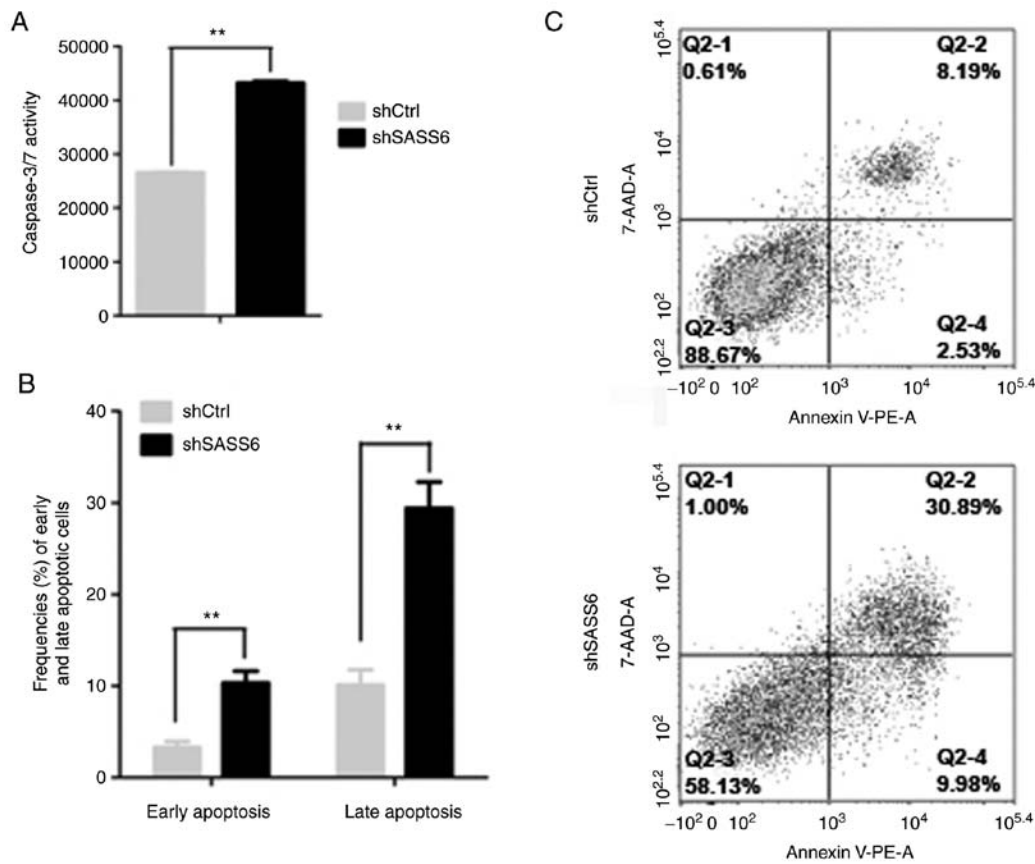


Figure 6. SASS6 knockdown induces apoptosis of MDA-MB-231 cells. (A) MDA-MB-231 cells were infected with the shCtrl or shSASS6 lentivirus and 3 days later, the Caspase3/7 activity in cells infected with shSASS6 was significantly higher compared with shCtrl-infected cells. \*\* $P < 0.01$ . (B) MDA-MB-231 cells were infected with shCtrl or shSASS6 and 4 days later, flow cytometric analysis of MDA-MB-231 cells stained with propidium iodide and Annexin V was performed. Results are presented as the percentage of cells in early and late apoptosis compared with the untreated controls. \*\* $P < 0.01$ . (C) Representative images of flow cytometric results are presented. SASS6, spindle assembly abnormal protein 6 homolog; sh, short hairpin; Ctrl, control.

## Discussion

Ectopic expression of SASS6 induces centrosome amplification, mitotic abnormalities, and chromosomal instability (9,10,12,17). SASS6 upregulation has been revealed in several different types of cancer (12). Despite extensive research on its role in centriole formation, the regulatory mechanism of SASS6 in the proliferation of human cancer cells remains to be elucidated. In the present study, SASS6 expression was upregulated in TNBC tissues and cells. To determine the effect of SASS6 in TNBC cells, SASS6 expression was knocked down in MDA-MB-231 TNBC cells, and the results revealed that SASS6 knockdown significantly inhibited proliferation of the MDA-MB-231 cells and arrested cell cycle progression at the G2/M phase.

During physiological cell proliferation, SASS6 serves an important role in the regulation of the centrosome numbers along with other proteins (17-22). Proliferating cells have a single centrosome, which is replicated once per cell cycle producing two centrosomes, and this guides the assembly of bipolar spindles during mitosis, thus ensuring accurate faithful separation of genetic material. Failure of centrosome replication can lead to the assembly of unipolar spindles. SASS6 levels must be limited to restrict procentriole formation to a single event per cell cycle (11); thus, overexpression of SASS6 in cancer may result in the formation of more than one

procentriole per cell cycle leading to abnormal cell proliferation, whereas downregulated expression of SASS6 levels may result in monopolar spindles, thus preventing cell proliferation. The results of the present study revealed that knockdown of SASS6 inhibited the proliferation of TNBC cells, suggesting that SASS6 may be a potential target for treatment of TNBC. Furthermore, the results revealed that the proportion of cells in the G1 phase of the SASS6-knockdown group was decreased, whereas the proportion of cells in the G2/M phase was significantly increased. Following knockdown of SASS6 in HeLa cells using siRNA, 53% of cells contained a single centrin focus; and 66% of this subset of cells assembled a monopolar spindle single centrin focus (11). Inhibition of SASS6 protein may result in the formation of a single centrin focus and thus inhibit spindle formation, leading to G2/M blockade, resulting in 4 or more chromosomes at the G2/M phase. It has been reported that SASS6 expression was detected at centrioles and in the cytoplasm of S-phase cells, and accumulated further in the cytoplasm as cells progressed through the G2 phase and until mitosis occurred (11). Knockdown of SASS6 in the present study resulted in G2/M phase arrest, further supporting the role of SASS6 as a mediator during the G2 phase of the cell cycle. Furthermore, due to G2/M blockade, cell proliferation in the experimental group was reduced, resulting in the proportion of cells in the G1 phase being significantly lower than the control group. The experimental results revealed that the SASS6 gene



acts in the mitosis phase of the cell cycle, which is consistent with the results of a previous study (11). The molecular mechanism of G2/M cell cycle arrest induced by knockdown of SASS6 in MDA-MB-231 cells was further assessed. The results revealed that the protein expression levels of CDK1 and cyclin B1 were downregulated following knockdown of SASS6. As CDK1 and cyclin B1 are two specific regulators that act during the G2/M phase, their expression was assessed. The results revealed that CDK1 and cyclin B1 may have been involved in the G2/M cell cycle arrest following knockdown of SASS6 in MDA-MB-231 cells. Moreover, shSASS6-treated cells exhibited downregulated expression of PCNA. PCNA serves an important role in the replisome by accommodating multiple processes at the replication fork in the G1-S phase (23). SASS6 expression was detected at centrioles and in the cytoplasm of S-phase cells as well, thus knockdown of SASS6 may regulate PCNA expression; however, the specific mechanism requires further study.

To further clarify the molecular mechanisms by which SASS6 suppressed breast cancer cell growth, phosphorylation of intracellular signal molecules in MDA-MB-231 cells was assessed following SASS6 knockdown. STAT3 is an oncogene and its constitutive activity can mediate the transformation of oncogenes (24). Constitutive activation of STAT3 signaling also confers resistance to apoptosis in cancer cells (25,26). Inhibition of the STAT3 signaling pathway can suppress the proliferation of ovarian and breast cancer cells which possess active STAT3 (27). It has been reported that STAT3 is constitutively activated in several different types of cancer, including breast cancer (28), although the mechanism underlying its activation requires further study. In the present study, it was revealed that knockdown of SASS6 decreased the levels of STAT3-Thr705 in human TNBC cells, suggesting that SASS6 is involved in activation of STAT3. Inhibition of STAT3 phosphorylation has been revealed to be associated with downregulation of CDK1 and cyclin B1 expression (29), thus it was concluded that knockdown of SASS6 may inhibit phosphorylation of STAT3, and this resulted in downregulation of CDK1 and cyclin B1, ultimately leading to G2/M blockade. In addition, phosphorylation of rpS6 can regulate translation initiation of certain mRNAs (30). Phosphorylation of rpS6 serves critical roles in neoplastic transformation and initiation of pancreatic cancer (31), dephosphorylation of rpS6 at Ser235/236 can decrease proliferation and cell motility, and invasion of breast cancer cells and pancreatic cancer cells (32); however, its function requires further study. The results of the present suggested that SASS6 knockdown significantly inhibited the growth of breast cancer cells by blocking the activation of STAT3 and rpS6 proteins.

BAD is a proapoptotic Bcl-2 family member, and the first cell death component identified as a survival signal regulatory target. Dephosphorylated BAD forms a heterodimer with Bcl-2 and Bcl-xL, inactivating them and thus allowing Bax and Bak proapoptotic members to form complexes, resulting in the release of cytochrome *c*, caspase activation and initiation of apoptosis (33-35). In the present study, SASS6 knockdown resulted in dephosphorylation of BAD.

The present study has some limitations. The possible effects of inhibition of SASS6 in animal models were not assessed to

observe whether it exhibited the same effects. Additionally, the use of cell lines may not be representative, as different cell line models may provide differing results.

In summary, the results of the present study revealed for the first time that SASS6 protein expression was upregulated in TNBC tumor tissues. Additionally, SASS6 knockdown inhibited TNBC cell growth and G2/M phase arrest through cyclin B1/CDK1 signaling and regulation of phosphorylation of STAT3, BAD and rpS6 protein. These data indicated that SASS6 may serve as a potential therapeutic target and merits further investigation in animal models or preclinical and clinical studies.

## Acknowledgements

The authors would like to thank Shanghai GeneChem Co., Ltd. for technical support.

## Funding

The present study was funded in part by the National Natural Science Foundation of China (grant no. 81573005), the Science and Technology Program of Shanxi Provincial Health Commission (grant no. 2017083), the Research Foundation of Capital Institute of Pediatrics (grant no. GZ-2021-11) and the Capital Institute of Pediatrics funds (grant no. FX-2016-03).

## Availability of data and materials

The datasets used and/or analyzed during the present study are available from the corresponding author on reasonable request.

## Authors' contributions

LD, JJ and HC conceived and designed the study, and participated in writing the manuscript. LD, YW, WW and XX performed the molecular genetics studies, and participated in the sequence alignment. YS and BT performed the cell culture. TS, CH and XZ analyzed and interpreted the data. All authors read and approved the final manuscript.

## Ethics approval and consent to participate

The present study was approved by the Ethics Committee of Shanxi Cancer Hospital (Shanxi, China). All patients provided informed consent for publication of their data.

## Patient consent for publication

Not applicable.

## Competing interests

The authors declare that they have no competing interests.

## References

- Sharma P: Update on the treatment of early-stage triple-negative breast cancer. *Curr Treat Options Oncol* 19: 22, 2018.

2. De Laurentiis M, Cianniello D, Caputo R, Stanzone B, Arpino G, Cinieri S, Lorusso V and De Placido S: Treatment of triple negative breast cancer (TNBC): Current options and future perspectives. *Cancer Treat Rev* 36 (Suppl 3): S80-S86, 2010.
3. Rivera-Rivera Y and Saavedra HI: Centrosome-a promising anti-cancer target. *Biologics* 10: 167-176, 2016.
4. Raff JW: Centrosomes and cancer: Lessons from a TACC. *Trends Cell Biol* 12: 222-225, 2002.
5. Salisbury JL: The contribution of epigenetic changes to abnormal centrosomes and genomic instability in breast cancer. *J Mammary Gland Biol Neoplasia* 6: 203-212, 2001.
6. Korzeniewski N, Hohenfellner M and Duensing S: The centrosome as potential target for cancer therapy and prevention. *Expert Opin Ther Targets* 17: 43-52, 2013.
7. Chan JY: A clinical overview of centrosome amplification in human cancers. *Int J Biol Sci* 7: 1122-1144, 2011.
8. Pihan GA, Purohit A, Wallace J, Knecht H, Woda B, Quesenberry P and Doxsey SJ: Centrosome defects and genetic instability in malignant tumors. *Cancer Res* 58: 3974-3985, 1998.
9. Leidel S, Delattre M, Cerutti L, Baumer K and Gönczy P: SAS-6 defines a protein family required for centrosome duplication in *C. elegans* and in human cells. *Nat Cell Biol* 7: 115-125, 2005.
10. Yoshida S, Tsuchiya Y, Ohta M, Gupta A, Shiratsuchi G, Nozaki Y, Ashikawa T, Fujiwara T, Natsume T, Kanemaki MT and Kitagawa D: HsSAS-6-dependent cartwheel assembly ensures stabilization of centriole intermediates. *J Cell Sci* 132: jcs217521, 2019.
11. Strnad P, Leidel S, Vinogradova T, Euteneuer U, Khodjakov A and Gönczy P: Regulated HsSAS-6 levels ensure formation of a single procentriole per centriole during the centrosome duplication cycle. *Dev Cell* 13: 203-213, 2007.
12. Shimura K, Kato H, Kawanishi Y, Nagura K, Kamo T, Okubo Y, Inoue Y, Kurabe N, Du C, Iwazumi M, *et al*: SASS6 overexpression is associated with mitotic chromosomal abnormalities and a poor prognosis in patients with colorectal cancer. *Oncol Rep* 34: 727-38, 2015.
13. Annika W, Anja MB, Kereshmeh T, Justus PB, Paul DD, Michael S, Raymund EH, Matthias WB, Pamela LS and Reiner S: Selective isolation and characterization of primary cells from normal breast and tumors reveal plasticity of adipose derived stem cells. *Breast Cancer Res* 18: 32, 2016.
14. Livak KJ and Schmittgen TD: Analysis of relative gene expression data using real-time quantitative PCR and the 2(-Delta Delta C(T)) method. *Methods* 25: 402-408, 2001.
15. Borroni C, Borroni E and Follenzi A: Lentiviral vector interactions with the host cell. *Curr Opin Virol* 21: 102-108, 2016.
16. Zha J, Harada H, Osipov K, Jockel J, Waksman G and Korsmeyer SJ: BH3 domain of BAD is required for heterodimerization with BCL-XL and pro-apoptotic activity. *J Biol Chem* 26: 272: 24101-24104, 1997.
17. Comartin D, Gupta GD, Fussner E, Coyaude É, Hasegan M, Archinti M, Cheung SW, Pinchev D, Lawo S, Raught B, *et al*: CEP120 and SPICE1 cooperate with CPAP in centriole elongation. *Curr Biol* 23: 1360-1366, 2013.
18. Xu X, Huang S, Zhang B, Huang F, Chi W, Fu J, Wang G, Li S, Jiang Q and Zhang C: DNA replication licensing factor Cdc6 and Plk4 kinase antagonistically regulate centrosome duplication via Sas-6. *Nat Commun* 8: 15164, 2017.
19. Arquint C, Sonnen KF, Stierhof YD and Nigg EA: Cell-cycle-regulated expression of STIL controls centriole number in human cells. *J Cell Sci* 125: 1342-1352, 2012.
20. Lin YC, Chang CW, Hsu WB, Tang CJ, Lin YN, Chou EJ, Wu CT and Tang TK: Human microcephaly protein CEP135 binds to hSAS-6 and CPAP, and is required for centriole assembly. *EMOJ* 32: 1141-1154, 2013.
21. Puklowski A, Homsy Y, Keller D, May M, Chauhan S, Kossatz U, Grünwald V, Kubicka S, Pich A, Manns MP, *et al*: The SCF-FBXW5 E3-ubiquitin ligase is regulated by PLK4 and targets HsSAS-6 to control centrosome duplication. *Nat Cell Biol* 13: 1004-1009, 2011.
22. Keller D, Orpinell M, Olivier N, Wachsmuth M, Mahen R, Wyss R, Hachet V, Ellenberg J, Manley S and Gönczy P: Mechanisms of HsSAS-6 assembly promoting centriole formation in human cells. *J Cell Biol* 204: 697-712, 2014.
23. Johnson A and O'Donnell M: Cellular DNA replicases: Components and dynamics at the replication fork. *Annu. Rev. Biochem* 74: 283-315, 2005.
24. Bromberg JF, Wrzeszczynska MH, Devgan G, Zhao Y, Pestell RG, Albanese C and Darnell JE Jr: Stat3 as an oncogene. *Cell* 98: 295-303, 1999.
25. William MB, Jin XH, Lin HJ, Huang M, Liu R, Reynolds RK and Lin J: Inhibition of constitutively active Stat3 suppresses growth of human ovarian and breast cancer cells. *Oncogene* 20: 7925-7934, 2001.
26. Catlett-Falcone R, Landowski T, Oshiro M, Turkson J, Levitzki A, Savino R, Ciliberto G, Moscinski L, Fernández-Luna JL, Nuñez G, *et al*: Constitutive activation of Stat3 signaling confers resistance to apoptosis in human U266 myeloma cells. *Immunity* 10: 105-115, 1999.
27. Shen Y, Devgan G, Darnell JE Jr and Bromberg JF: Constitutively activated Stat3 protects fibroblasts from serum withdrawal and UV induced apoptosis and antagonizes the proapoptotic effects of activated Stat1. *Proc Natl Acad Sci USA* 98: 1543-1548, 2001.
28. Garcia R, Yu CL, Hudnall A, Catlett R, Nelson KL, Smithgall T, Fujita DJ, Ethier SP and Jove R: Constitutive activation of Stat3 in fibroblasts transformed by diverse oncoproteins and in breast carcinoma cells. *Cell Growth Differ* 8: 1267-1276, 1997.
29. Roshan S, Liu YY, Banafa A, Chen HJ, Li KX, Yang GX, He GY and Chen MJ: Fucoidan induces apoptosis of HepG2 cells by down-regulating p-Stat3. *J Huazhong Univ Sci Technolog Med Sci* 34: 330-336, 2014.
30. Roux PP, Shahbazian D, Vu H, Holz MK, Cohen MS, Taunton J, Sonenberg N and Blenis J: RAS/ERK signaling promotes site-specific ribosomal protein S6 phosphorylation via RSK and stimulates cap-dependent translation. *J Biol Chem* 282: 14056-14064, 2007.
31. Meyuhas O: Ribosomal protein S6 phosphorylation: Four decades of research. *Int Rev Cell Mol Biol* 320: 41-73, 2015.
32. Akar U, Ozpolat B, Mehta K, Lopez-Berestein G, Zhang D, Ueno NT, Hortobagyi GN and Arun B: Targeting p70S6K prevented lung metastasis in a breast cancer xenograft model. *Mol Cancer Ther* 9: 1180-1187, 2010.
33. Zha J, Harada H, Yang E, Jockel J and Korsmeyer SJ: Serine phosphorylation of death agonist BAD in response to survival factor results in binding to 14-3-3 not BCL-X(L). *Cell* 87: 619-628, 1996.
34. Yang E, Zha J, Jockel J, Boise LH, Thompson CB and Korsmeyer SJ: Bad, a heterodimeric partner for Bcl-XL and Bcl-2, displaces Bax and promotes cell death. *Cell* 80: 285-291, 1995.
35. Wei MC, Zong WX, Cheng EH, Lindsten T, Panoutsakopoulou V, Ross AJ, Roth KA, MacGregor GR, Thompson CB and Korsmeyer SJ: Proapoptotic BAX and BAK: A requisite gateway to mitochondrial dysfunction and death. *Science* 292: 727-730, 2001.